



Hydration kinetics modeling of Portland cement considering the effects of curing temperature and applied pressure

Feng Lin^{a,b,*}, Christian Meyer^a

^a Department of Civil Engineering and Engineering Mechanics, Columbia University, New York, NY 10027, USA

^b Department of Civil Engineering, Tsinghua University, Beijing 100084, China

ARTICLE INFO

Article history:

Received 7 November 2006

Accepted 28 January 2009

Keywords:

Hydration

Kinetics

Portland cement

Modeling

Thermodynamics

ABSTRACT

A hydration kinetics model for Portland cement is formulated based on thermodynamics of multiphase porous media. The mechanism of cement hydration is discussed based on literature review. The model is then developed considering the effects of chemical composition and fineness of cement, water–cement ratio, curing temperature and applied pressure. The ultimate degree of hydration of Portland cement is also analyzed and a corresponding formula is established. The model is calibrated against the experimental data for eight different Portland cements. Simple relations between the model parameters and cement composition are obtained and used to predict hydration kinetics. The model is used to reproduce experimental results on hydration kinetics, adiabatic temperature rise, and chemical shrinkage of different cement pastes. The comparisons between the model reproductions and the different experimental results demonstrate the applicability of the proposed model, especially for cement hydration at elevated temperature and high pressure.

© 2009 Elsevier Ltd. All rights reserved.

1. Introduction

The hydration of cement and the accompanying phenomena such as heat generation, strength development and shrinkage are the results of interrelated chemical, physical and mechanical processes. A thorough understanding of these processes is a critical prerequisite for modeling hydration kinetics of cementitious materials.

The advances of computer technology made it possible for a branch of computational materials science to develop rapidly in the past twenty years, i.e., the computer modeling of hydration and microstructure development of concrete. Noteworthy studies include those of Jennings and Johnson [1], Bentz and Garboczi [2], van Breugel [3], Navi and Pignat [4], and Maekawa et al. [5]. Among these, the NIST model, referred to as CEMHYD3D [6], and the HYMOSTRUC model [3] appear to be the most advanced and widely used ones. These models attempt to simulate cement hydration and microstructure formation on the elementary level of cement particles, which is the most rational way, as long as the chemical, physical and mechanical characteristics of cement hydration are properly taken into account.

However, there exist certain applications for which simpler mathematical models describing and quantifying hydration kinetics are necessary. In fact, numerous attempts have been undertaken with that objective and many such simplified formulations can be found in

the literature, e.g., Byfors [7], Knudsen [8], Freiesleben Hansen and Pedersen [9], Basma et al. [10], Nakamura et al. [11], Cervera et al. [12], Schindler and Folliard [13], and Bentz [14]. In contrast to the aforementioned microscopic models, most of these simplified models are empirical in nature, based on experimental observations of macroscopic phenomena, and they capture the effects of curing temperature, water–cement ratio, fineness, particle size distribution and chemical composition of cement with different degrees of accuracy. The range of curing temperature in these models is usually small and does not exceed 60 °C, and none of them include the effect of applied pressure. However, elevated temperatures and high pressures are frequently encountered in oil wells where they must be addressed.

In this study, a hydration kinetics model is formulated based on the thermodynamics of multiphase porous media, which was first proposed by Ulm and Coussy [15]. The hardening cement paste is known to be a multiphase porous material and the thermodynamics theory of [15] is an ideal framework to model hydration kinetics. Cervera et al. [12,16] proposed an equation to describe hydration kinetics using this theory, but it needs to be elaborated and reformulated to take into account the experimental observations of cement hydration, especially curing temperature and applied hydrostatic pressure. This paper presents the theoretical formulation of a new model. The model parameters are calibrated and related to the chemical composition of cement through simple but explicit equations; the model is then used to predict the experimental results of different investigators, including those on hydration kinetics, adiabatic temperature rise, and chemical shrinkage of cement pastes.

* Corresponding author. Department of Civil Engineering and Engineering Mechanics, Columbia University, New York, NY 10027, USA.

E-mail address: fl2040@columbia.edu (F. Lin).

2. Literature survey on hydration of Portland cement

Before a mathematical model can be developed that properly considers the various influencing factors, the known facts of Portland cement hydration should be thoroughly surveyed. A comprehensive study on cement hydration was conducted by van Breugel [3]. However, during the past decades, many new findings, mostly experimental, regarding cement hydration have been reported. Therefore, the most recent findings and their relevance to understand Portland cement hydration will be addressed herein.

2.1. Influence of chemical composition of cement

The composition of cement is the most important influencing factor of all. There exist two forms in which to describe the composition of cement, i.e. the oxide composition and the chemical composition. The latter is usually determined using the compound stoichiometries and the values of the former. The Bogue calculation [17] is the most frequently quoted mathematical procedure among such indirect methods and thus is used in the present study.

Experimental results show that the four major clinker phases of cement, viz. C_3S , C_2S , C_3A and C_4AF have different reaction rates with water [18–20]. It is well known that C_3A reacts the fastest, followed by C_3S and the other two. However, whether the individual constituent phases hydrate independently from one another or at equal fraction rates is still not resolved [3]. Because of different reaction rates of the clinker phases and their interactions, it is generally accepted that the so-called degree of hydration of cement is just an overall and approximate measure. Due to the difficulty of identifying and simulating the complicated interactions, the overall degree of hydration, denoted as α , is still widely used [1–16] and will be employed in this study.

2.2. Influence of water–cement ratio

The water–cement ratio, $\frac{w}{c}$, also influences hydration kinetics. Experimental results have shown that a higher water–cement ratio leads to a higher hydration rate after the middle period of hydration, but only has a small effect on the hydration rate in the early stage [21,22]. The water–cement ratio also determines the ultimate degree of hydration α_u . Theoretically, a water–cement ratio of about 0.4 is sufficient for the complete hydration of cement (i.e. $\alpha_u = 1.0$). In other words, a water–cement ratio higher than 0.4 will lead to full hydration given enough time. However, cement hydration is retarded at low internal relative humidity, and the theoretical water–cement ratio of about 0.4 is not sufficient for full hydration [23]. The hydration products around the anhydrous cement particles prevent further hydration if there is insufficient free water in the macro-pores. From experimental observations, the relationship between the ultimate degree of hydration α_u and the water–cement ratio can be described by a hyperbola with $\alpha_u \leq 1.0$. Mills [24] conducted a series of tests and derived the following equation for α_u ,

$$\alpha_u = \frac{1.031 \frac{w}{c}}{0.194 + \frac{w}{c}} \leq 1.0 \quad (1)$$

This equation has been used frequently in hydration kinetics modeling [13]. However, it does not consider the effects of cement fineness and curing temperature and may underestimate the ultimate degree of hydration in some cases.

2.3. Influence of fineness of cement

The fact that fineness of cement influences the ultimate degree of hydration α_u as well as the hydration rate has been observed in experiments and numerical simulations [25,26]. The finer the cement particles, the higher α_u , and the higher the hydration rate. However,

Bentz and Haecker [26] also found that at low water–cement ratios, the influence of cement fineness on α_u diminishes. A finer cement, or cement with a larger surface area, provides a larger contact area with water and hence causes a higher hydration rate. Also, at the same degree of hydration, a larger surface area corresponds to a smaller thickness of hydration products around the anhydrous cement particles, which increases the ultimate degree of hydration. Apart from fineness, the particle size distribution of cement also influences the hydration rate [3,8,27,28].

2.4. Influence of curing temperature

The effects of curing temperature on hydration kinetics have been shown to be twofold. On the one hand, the reaction rate α increases with the increase in temperature [29–31]. On the other hand, the density of hydration products at higher temperature is higher [32], which slows down the permeation of free water through the hydration products. Therefore, during the late period, the hydration rate is lower at elevated temperature and the ultimate degree of hydration may thus also be lower. Based on the experimental results in [32], van Breugel [3] proposed the following equation for the volume ratio between hydration products and the reacted cement at temperature T [K]:

$$v(T) = \frac{\text{Volume of Hydration Products at } T}{\text{Volume of Reacted Cement at } T} = v_{293} \exp[-28 \times 10^{-6}(T - 293)^2] \quad (2)$$

Generally, $v_{293} \approx 2.2$ according to Powers and Brownard [33].

It should be pointed out that the available experimental results regarding the effects of elevated curing temperature on hydration kinetics are still very limited. Very few publications can be found that consider curing temperatures higher than 60 °C (333 K). Chenevert and Shrestha [34] and Hills et al. [35] are the two studies worth mentioning.

An issue related to the effects of curing temperature is the apparent activation energy E_a . Because cement is a mixture of different chemical components rather than a pure material, its activation energy is merely phenomenological and can only be referred to as the apparent one. Different and conflicting conclusions regarding the value of the apparent activation energy have been drawn based on experiments and theoretical analysis. Xiong and van Breugel [3,36] argued that E_a is a function of chemical composition of cement, curing temperature and the degree of hydration. Freiesleben Hansen and Pedersen [37], on the other hand, suggested that E_a is only a function of curing temperature. Schindler [38] proposed an equation for E_a that considers the chemical composition and fineness of cement. Among these studies, the work of [38] is found to be most convincing because of its applicability to a wide range of cements and simplicity.

2.5. Influence of applied pressure

The experiments to investigate the influence of applied pressure on hydration kinetics are even scarcer than those involving curing temperatures. Roy et al. [39,40] studied strength development of cement pastes at high temperature and high pressure, but did not address hydration kinetics. Bresson et al. [41] conducted hydration tests on C_3S subject to hydrostatic pressure up to 85 MPa and found that a higher pressure increases hydration rate. Zhou and Beaudoin [42] also found that applied hydrostatic pressure increases the hydration rate of Portland cement, but has only a negligible effect on the pore structure of hydration products when different cement pastes at similar degrees of hydration are compared. The finding of [42] is important since it implies that the density of the hydration products is not considerably affected by the applied hydrostatic pressure, at least not up to 6.8 MPa, which is the pressure they used.

2.6. Mechanisms and thermo-chemical concepts of cement hydration

Based on numerous experimental observations, the mechanism of cement hydration is fairly clear. According to [3], it involves three main stages, viz. the early, middle and late periods. A short period of rapid chemical dissolution, termed the pre-induction period, is followed by a dormant stage, which lasts for several hours. Then cement hydration enters the middle period that can last for 24 to 48 h, in which ions transport to and from the surfaces of anhydrous cement particles through gradually growing layers of hydration products. During the late period, which is the longest and dominant one, the reaction is totally diffusion-controlled. The free water in macro-pores permeates through the hydration products formed around the anhydrous cement core, making further reactions possible. van Breugel [3] claims that cement hydration follows two different mechanisms at different stages. During the early and middle periods, the phase boundary mechanism prevails, while in the late period, the diffusion-controlled reaction dominates. However, it is very difficult to define a definite boundary between the two mechanisms.

In the present study, it is assumed that the phase boundary mechanism can be regarded as a special case of the diffusion-controlled reaction when the layers of hydration products around the anhydrous cement cores are very thin. The mechanisms of cement hydration are then unified to be the diffusion-controlled one. Cement hydration is interpreted as a chemical reaction in which the free water in the macro-pores combines as a reactant phase with the anhydrous cement and becomes the chemically bound water as a product phase, and the dominant mechanism of the reaction kinetics is the diffusion of free water through layers of hydration products, as illustrated in Fig. 1 [15]. The assumption can simplify the model formulation yet still capture the salient feature of cement hydration.

Using the thermodynamics of reactive porous media and assuming a closed system, the thermodynamic inequality equation can be expressed as [15]:

$$\sigma_{ij}\dot{\varepsilon}_{ij} - S\dot{T} - \dot{\Psi} + \Phi_{A \rightarrow B} \geq 0 \tag{3}$$

in which σ_{ij} is the ij th component of the stress tensor, ε_{ij} is the ij th component of the strain rate tensor, S is the entropy, \dot{T} is the variation rate of temperature, $\dot{\Psi}$ is the variation rate of free energy, and $\Phi_{A \rightarrow B}$ is the dissipation associated with the chemical reaction $A \rightarrow B$. For cement hydration, according to the aforementioned mechanism, A is the free water in macro-pores and B is the chemically bound water in hydration products. The chemical dissipation $\Phi_{A \rightarrow B}$ can be expressed as:

$$\Phi_{A \rightarrow B} = A_\alpha \dot{\alpha} \geq 0 \tag{4}$$

where A_α is the affinity of the chemical reaction $A \rightarrow B$, viz. the chemical affinity of cement hydration, and $\dot{\alpha}$ is the reaction rate, i.e.

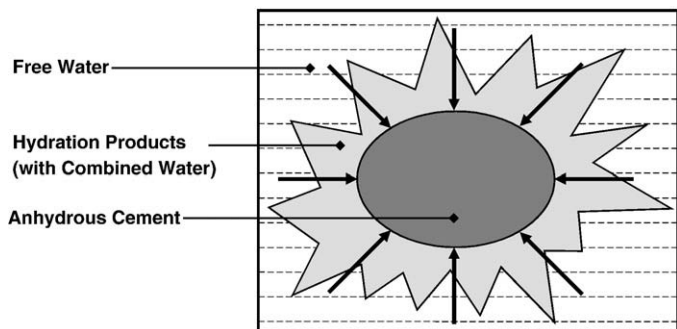


Fig. 1. Diffusion of free water through layers of hydration products [15].

the variation rate of the degree of hydration. Using the Arrhenius equation, the chemical affinity A_α can be written as:

$$A_\alpha = \frac{\dot{\alpha}}{\eta_\alpha} \exp\left(\frac{E_\alpha}{RT}\right) \tag{5}$$

in which η_α represents the permeability of the hydration products around the anhydrous cement, E_α is the apparent activation energy, R is the universal gas constant, and T is the absolute temperature. The apparent activation energy E_α is used in Eq. (5) because as pointed out in [3], it is an experimentally obtained quantity that is a net result of the temperature dependency of several processes.

With Eq. (5), the hydration rate $\dot{\alpha}$ can be written as:

$$\dot{\alpha} = A_\alpha \eta_\alpha \exp\left(-\frac{E_\alpha}{RT}\right) \tag{6}$$

Eq. (6) provides an ideal framework for the modeling of hydration kinetics of cement, provided the factors that influence the chemical affinity A_α and the permeability η_α can be identified and quantified.

3. Model formulation

3.1. Modeling of the influence factors

It is obvious that the chemical composition of cement affects both the chemical affinity A_α and the permeability η_α , whereas the water–cement ratio influences only the chemical affinity A_α , since it determines the chemical potential of free water in the multiphase system of cement paste to a certain extent.

The following expression may be used to relate the chemical affinity A_α to the chemical composition of cement and water–cement ratio [12]:

$$A_\alpha \propto k \left(\frac{A_0}{k\alpha_u} + \alpha \right) (\alpha_u - \alpha) \tag{7}$$

in which \propto means proportional to, k and A_0 are parameters related to the chemical composition of cement and other factors. A_0 is actually the initial chemical affinity of cement hydration ($\alpha=0$). Eq. (7) implicitly considers the so-called water shortage effect as pointed out in [3], since the ultimate degree of hydration α_u is affected by the water–cement ratio.

From Eq. (6), it can be seen that the effects of A_α and η_α are demonstrated through their products. In order to simplify the model, an exponential equation is used to represent the permeability η_α that is:

$$\eta_\alpha = \exp(-n\alpha) \tag{8}$$

in which n is a parameter that depends on curing temperature, degree of hydration, and fineness of cement. η_α can be considered the normalized permeability, which means all the model coefficients are taken into account by A_α . Eq. (8) describes the gradual decrease in permeability of hydration products with the development of hydration. In fact, the exponential function has been frequently used to describe hydration kinetics [12,13].

According to Eqs. (7) and (8), the chemical composition of cement influences the three parameters, k , A_0 and n , while the water–cement ratio affects only α_u . With different values of α_u , Eqs. (6)–(8) reflect implicitly the effects of water–cement ratio on hydration rate.

For the sake of simplicity, only the fineness of cement particles but not the actual particle size distribution is taken into account in the present model. Since for most general-purpose Portland cements, the shapes of their particle size distribution curves are similar, this simplification does not introduce significant errors. The fineness of cement can be represented by the Blaine value with units of m^2/kg . It influences the initial reaction rate of cement. Therefore, it should

appear in the expression for the parameter A_0 , which represents the initial chemical affinity of cement hydration. Hence the following equation is used to express A_0 :

$$A_0 = \frac{A'_0 \times \text{Blaine}}{350} \quad (9)$$

in which A'_0 is the normalized initial chemical affinity of cement hydration and is only a function of the chemical composition of cement.

The *Blaine* fineness also affects the permeability η_α and the ultimate degree of hydration α_u . For permeability, it is noticed that the finer the cement particles, the larger the *Blaine* value, the thinner the layers of the hydration products, hence the higher the permeability of the hydration products and the smaller the parameter n (Eq. (8)). Therefore, it is assumed that:

$$n \propto 1 + (1 - \alpha)^2 \ln \frac{350}{\text{Blaine}} \quad (10)$$

As can be seen in Eq. (10), the effect of *Blaine* fineness is not constant throughout the hydration process. With an increase in the degree of hydration α , the effect of *Blaine* fineness decreases.

The effects of curing temperature can be considered partly by involving one term of the Arrhenius equation, as shown in Eq. (6). However, the densifying effect of elevated curing temperature on the hydration products should also be considered. Since the density of the hydration products is closely related to the permeability η_α , the parameter n in Eq. (8) should also be a function of curing temperature. And since the hydration rate of cement during the late period decreases at elevated curing temperatures, the parameter n should be an increasing function of the curing temperature T . In this study, the volume ratio equation (Eq. (2)) is used, with the effect of curing temperature T on the parameter n represented as:

$$n \propto \left(\frac{v_{293}}{v(T)} \right)^{10\alpha^4} \quad (11)$$

in which α is the degree of hydration, and $v(T)$ and v_{293} are as given in Eq. (2). Eqs. (8) and (11) imply that the effect of curing temperature on the permeability η_α is a decreasing function of the degree of hydration α , which is consistent with experimental results [29–31]. The curing temperature T also influences the ultimate degree of hydration α_u , as will be discussed subsequently.

The applied hydrostatic pressure p is assumed to influence only the chemical affinity A_α , as supported by the experimental results in [42]. According to the tests conducted by Bresson et al. [41], the chemical affinity A_α is set to be:

$$A_\alpha \propto \exp \left\{ 0.02 \left(\frac{p}{p_{\text{atm}}} - 1 \right)^{0.07} \left[\frac{\alpha}{\alpha_u} - 1.5 \left(\frac{\alpha}{\alpha_u} \right)^2 + 0.4 \right] \right\} \quad (12)$$

where p is the applied hydrostatic pressure, and p_{atm} is the atmospheric pressure. Eq. (12) shows that the reaction rate increases with the increase in the applied pressure p .

It can be concluded now that the chemical affinity A_α is a function of the degree of hydration α , the water cement ratio $\frac{w}{c}$ (through the ultimate degree of hydration α_u), the *Blaine* fineness (through the initial chemical affinity A_0 and the ultimate degree of hydration α_u), the applied pressure p (through Eq. (12)), and the chemical composition of cement (through the parameters A'_0 and k). And the parameter n that controls the permeability of free water through the hydration products is a function of the curing temperature T (through Eq. (11)), the degree of hydration α , the *Blaine* fineness (through Eq. (10)), and the chemical composition of cement. Thus, if the ultimate degree of hydration α_u is identified, the parameters that

remain in the hydration kinetics model will be related to the chemical composition of cement only.

3.2. Modeling of the ultimate degree of hydration

The available experimental and numerically simulated results for α_u as a function of water–cement ratio and fineness of cement [22,24,43–45] were collected and analyzed. The *Blaine* fineness of the cements ranges from around 270 m²/kg to 420 m²/kg and the water–cement ratio varies from 0.25 to 0.85. For some sets of data, in which the hydration ages were not long enough, small extrapolations were performed based on the trends of the degree-of-hydration vs. time curves to obtain the corresponding ultimate degree of hydration. It must be pointed out that theoretically, the ultimate degree of hydration can never be obtained from experiments, since very limited reactions may still be possible after years. However, the very limited reactions at sufficiently late age are of little significance for practical application and the final degrees of hydration found in [22,24,43–45] are assumed to be the ultimate ones.

From the data analysis, it was found that:

- 1) The ultimate degree of hydration α_u may be expressed as a hyperbolic function of water–cement ratio with $\alpha_u \leq 1.0$.
- 2) α_u cannot exceed the theoretical value given by:

$$\alpha_u \leq \frac{w}{0.4c} \quad (13)$$

in which 0.4 is approximately the theoretical water–cement ratio necessary for full hydration, which is the sum of the chemically bound water ratio, about 0.25, and the gel water ratio, about 0.15 [3,33].

- 3) α_u increases as the cement particles get finer, i.e. as the *Blaine* value increases. The effect of cement fineness on α_u becomes smaller with a decrease in water–cement ratio [26].

Based on these observations, an equation considering both the effects of water–cement ratio and fineness of cement is obtained via theoretical analysis and data regression:

$$\alpha_{u,293} = \frac{\beta_1(\text{Blaine}) \times \frac{w}{c}}{\beta_2(\text{Blaine}) + \frac{w}{c}} \leq 1.0 \quad (14)$$

in which $\alpha_{u,293}$ is the ultimate degree of hydration at $T=293$ K, β_1 and β_2 are both functions of *Blaine* fineness and are defined as:

$$\beta_1(\text{Blaine}) = \frac{1.0}{9.33 \left(\frac{\text{Blaine}}{100} \right)^{-2.82} + 0.38} \quad (15)$$

$$\beta_2(\text{Blaine}) = \frac{\text{Blaine} - 220}{147.78 + 1.656(\text{Blaine} - 220)} \quad (16)$$

Eqs. (15) and (16) are valid for $\text{Blaine} \geq 270$ m²/kg. When $\text{Blaine} < 270$ m²/kg, β_1 and β_2 are assumed to remain constant, that is,

$$\beta_1(\text{Blaine} < 270 \text{ m}^2/\text{kg}) = \beta_1(\text{Blaine} = 270 \text{ m}^2/\text{kg}) \quad (17)$$

$$\beta_2(\text{Blaine} < 270 \text{ m}^2/\text{kg}) = \beta_2(\text{Blaine} = 270 \text{ m}^2/\text{kg}) \quad (18)$$

The applicability of the proposed equation for $\alpha_{u,293}$ is validated using the experimental results of Mills [24] and Baroghel-Bouny et al. [45], as shown in Fig. 2.

The ultimate degree of hydration α_u is also related to the curing temperature T . Based on the experimental results of Kjellsen and Detwiler [30] and Escalante-Garcia [31] for three different Portland

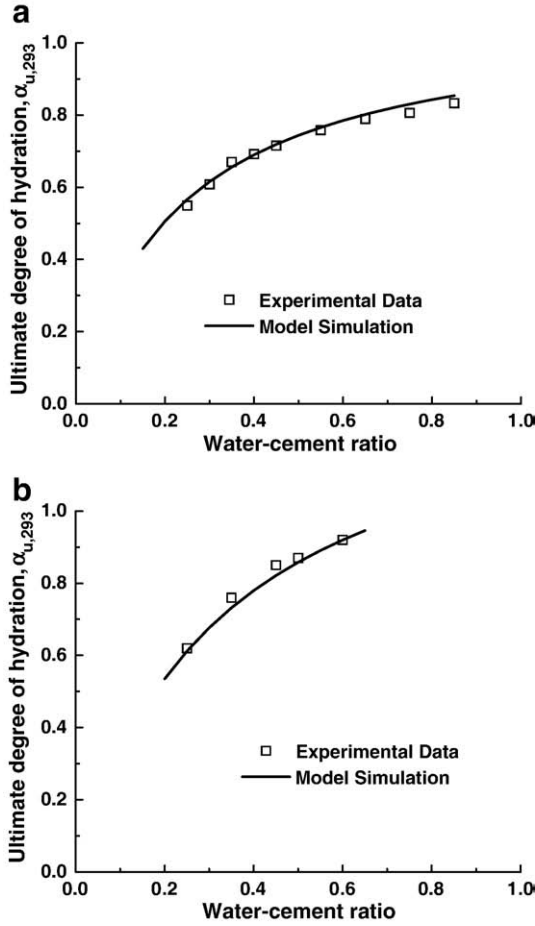


Fig. 2. Simulated and measured ultimate degree of hydration at $T=293$ K (a)—experimental data from [24]; (b)—experimental data from [45].

cements, the following equation is proposed to consider the effect of curing temperature T :

$$\alpha_u = \alpha_{u,293} \exp \left[-0.00003(T - 293)^2 \cdot \text{SGN}(T - 293) \right] \quad (19)$$

in which

$$\text{SGN}(T - 293) = \begin{cases} 1, & \text{when } T \geq 293\text{K} \\ -1, & \text{when } T < 293\text{K} \end{cases} \quad (20)$$

It should be noted that the equation for α_u must also be bounded by the theoretical value. When the water-cement ratio is low, α_u predicted by Eqs. (14)–(20) can be higher than the theoretical value of Eq. (13). Therefore, if the calculated α_u exceeds that theoretical value, it is assumed that:

$$\alpha_u = \frac{w}{0.4c} \quad (21)$$

3.3. Mathematical model of hydration kinetics

With the above discussion and formulation, a mathematical model of hydration kinetics for Portland cement can now be presented.

The rate of hydration $\dot{\alpha}$ is given by Eq. (6), but normalized, that is,

$$\dot{\alpha} = A_\alpha \eta_\alpha \exp \left(-\frac{E_a}{RT} \right) \exp \left(\frac{E_a}{293R} \right) \quad (22)$$

in which E_a is the apparent activation energy. The normalization in Eq. (22) ensures that the material constants of the model can be

obtained from experimental results at room temperature and will not vary considerably for different values of activation energy.

The chemical affinity A_α is expressed as:

$$A_\alpha \left(\alpha, \frac{w}{c}, \text{Blaine}, p \right) = k \left(\frac{A_0}{k\alpha_u} + \alpha \right) (\alpha_u - \alpha) \cdot s(\alpha, p) \quad (23)$$

in which the function $s(\alpha, p)$ represents the effect of applied hydrostatic pressure p (see also Eq. (12)):

$$s(\alpha, p) = \exp \left\{ 0.02 \left(\frac{p}{p_{\text{atm}}} - 1 \right)^{0.07} \left[\frac{\alpha}{\alpha_u} - 1.5 \left(\frac{\alpha}{\alpha_u} \right)^2 + 0.4 \right] \right\} \quad (24)$$

The initial chemical affinity A_0 is defined by Eq. (9), and the ultimate degree of hydration α_u is given by Eqs. (14)–(21). The remaining constants A_0 and k are functions of the chemical composition of cement.

The permeability of free water through hydration products, η_α is expressed by Eq. (8), in which the parameter n is written as:

$$n = n_0 f_1(\text{Blaine}, \alpha) \cdot f_2(T, \alpha) \quad (25)$$

where

$$f_1(\text{Blaine}, \alpha) = 1 + (1 - \alpha)^2 \cdot \ln \left(\frac{350}{\text{Blaine}} \right) \quad (26)$$

$$f_2(T, \alpha) = \left(\frac{V_{293}}{V(T)} \right)^{10\alpha^4} \quad (27)$$

and n_0 is a material constant that is related to the chemical composition of cement only.

The last material constant of this model is the apparent activation energy E_α . In this study, it is assumed that E_α is constant for one specific type of cement. The empirical equation obtained in [38] is used to determine E_α , which is a function of the chemical composition and fineness of cement.

4. Model calibration

The proposed model contains four material constants, k , A_0 , n_0 and the apparent activation energy E_α , all of which depend on the cement properties only. The first three are functions of the chemical composition of cement only, while the apparent activation energy depends also on the fineness of cement [38]. To calibrate these material constants, the experimental results on hydration kinetics for eight different Portland cements are used, namely those for Type I, Type II, Type III and Type IV cements of Lerch and Ford [29], and those of Keienburg [25], Danielson [21], Escalante-Garcia [31], and Taplin [22]. In Table 1, these cements are identified as #A–#H, respectively. The experimental results used cover the effects of curing temperature, water-cement ratio, and fineness of cement on hydration kinetics of Portland cement, with the mass fraction of C_3S in cement ranging from 0.24 to 0.717.

An equation was proposed in [38] for the apparent activation energy E_α [J/mol],

$$E_\alpha = 22100 \times (p_{C_3A})^{0.30} \times (p_{C_4AF})^{0.25} \times (\text{Blaine})^{0.35} \quad (29)$$

in which the *Blaine* fineness is with units of m^2/kg . p_{C_3A} and p_{C_4AF} are the Bogue mass fractions of C_3A and C_4AF , respectively. This equation is used in the present study to obtain the apparent activation energy if its value was not provided in the experimental data.

The Bogue compositions of the cements investigated are listed in Table 1. The four material constants are also shown for each cement. It can be seen from Eq. (22) that for experiments conducted at room

Table 1
Cement compositions and the corresponding material constants.

Cement identification #	Figure number	Bogue composition				Blaine fineness (m ² /kg)	Material constants			
		C ₃ S	C ₂ S	C ₃ A	C ₄ AF		E _α (J/mol)	k (h ⁻¹)	n ₀	A ₀ (h)
#A [29]	3-1	0.514	0.226	0.111	0.079	372	45,271 ^a	0.53	6.95	0.0123
#B [29]	3-2	0.416	0.344	0.054	0.132	314	41,788 ^a	0.48	7.30	0.0080
#C [29]	3-3	0.600	0.135	0.089	0.081	564	49,955 ^a	0.54	6.80	0.0120
#D [29]	3-4	0.240	0.515	0.049	0.116	360	39,978 ^a	0.50	7.30	0.0100
#E [25]	3-5	0.717	0.059	0.090	0.100	350	–	0.59	7.10	0.0108
#F [21]	3-6	0.567	0.172	0.067	0.079	312	–	0.51	7.00	0.0120
#G [31] ^b	3-7	0.716	0.109	0.037	0.107	376	44,166 ^c	0.47	8.10	0.0100
#H [22]	3-8	0.414	0.340	0.098	0.075	312	–	0.55	7.02	0.0130

^a Values taken from [38].

^b The chemical composition determined by quantitative X-ray diffraction analysis (QXDA) was used for this cement.

^c Calculated value using Eq. (29).

temperature, E_{α} is not significant for the model. The other three material constants are obtained by fitting the experimental data. The material constants are not necessarily the ones that best fit the experimental results, as they have been adjusted to allow for their variations with the chemical compositions by conducting linear or nonlinear regression analyses with EXCEL. The comparison of the model simulations with the experimental results for the eight cements are shown in Figs. 3–10, respectively.

The material constants k , A_0 and n_0 of Table 1 can be approximately represented by certain functions of the Bogue composition of cement.

The normalized initial affinity A_0 can be expressed as a linear function of the Bogue mass fractions of C₄AF. The experimental results of Escalante-García and Sharp [20] support this relation. It can be seen from their experimental data that the initial reaction rate of C₄AF is much lower than that of C₃S, C₂S and C₃A, which have similar initial reaction rates. The function of A_0 is expressed as:

$$A_0 = -0.0767p_{C_4AF} + 0.0184 \quad (30)$$

with p_{C_4AF} being the Bogue mass fraction of C₄AF. The comparison of A_0 calculated by Eq. (30) with the values listed in Table 1 is shown in Fig. 11(a).

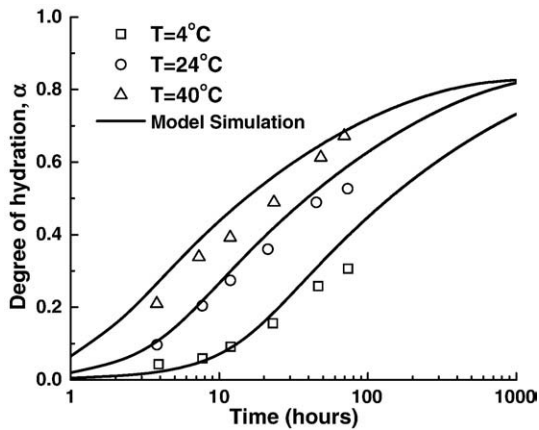


Fig. 3. Simulated and measured degree of hydration for cement #A (type I) (experimental data from [29]).

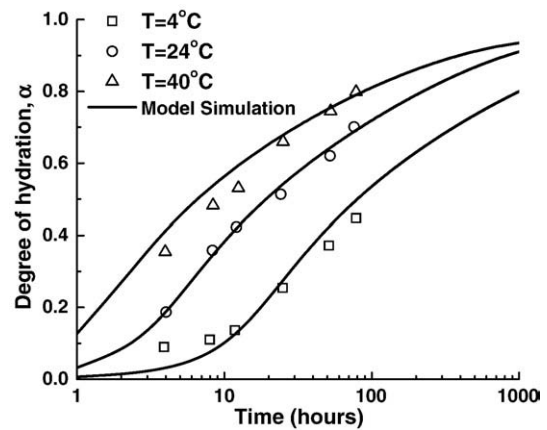


Fig. 5. Simulated and measured degree of hydration for cement #C (type III) (experimental data from [29]).

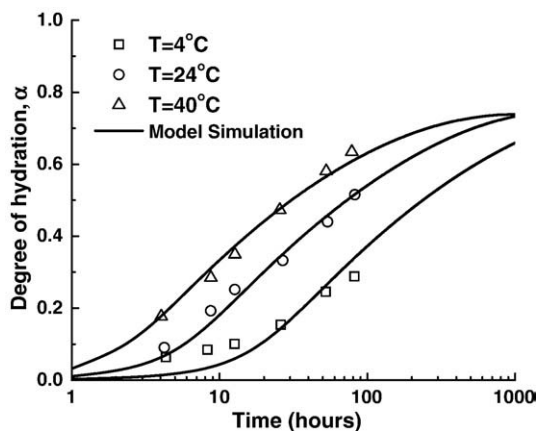


Fig. 4. Simulated and measured degree of hydration for cement #B (type II) (experimental data from [29]).

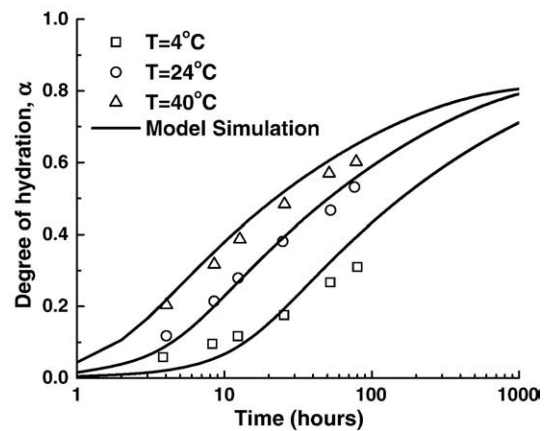


Fig. 6. Simulated and measured degree of hydration for cement #D (type IV) (experimental data from [29]).

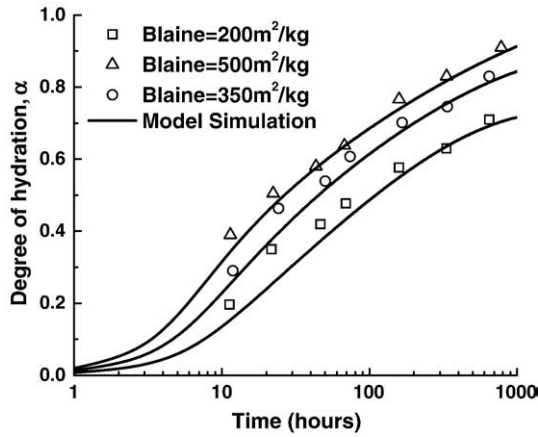


Fig. 7. Simulated and measured degree of hydration for cement #E (experimental data from [25]).

The constants n_0 and k can be represented by a linear and a nonlinear function of the Bogue mass fractions of C_3S , C_2S , and C_3A , respectively:

$$k = 0.56 \times (p_{C_3S})^{-0.206} \times (p_{C_2S})^{-0.128} \times (p_{C_3A})^{0.161} \quad (31)$$

$$n_0 = 10.945p_{C_3S} + 11.25p_{C_2S} - 4.10p_{C_3A} - 0.892 \quad (32)$$

The comparisons of k calculated by Eq. (31) and n_0 calculated by Eq. (32) with the values listed in Table 1 are shown in Fig. 11(b) and (c), respectively.

It can be seen in Fig. 11 that the three model parameters (k , A'_0 and n_0) correlate strongly with the chemical composition of cement. Although only eight cements were used for the data regression analysis, considering the fact that the chemical compositions of these cements are very different, the trends of the functional relationships appear to be captured very well.

5. Model verification

5.1. Model reproduction of the degree of hydration

In order to validate the proposed model, it is used to reproduce hydration kinetics for several cements.

First of all, the model capability to predict the degree of hydration of cement under pressure is verified using the experimental results. As

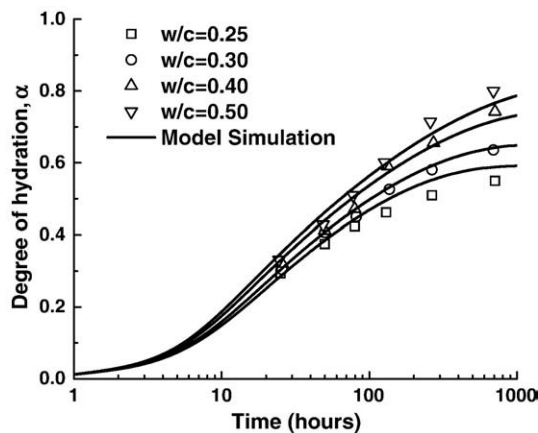


Fig. 8. Simulated and measured degree of hydration for cement #F (experimental data from [21]).

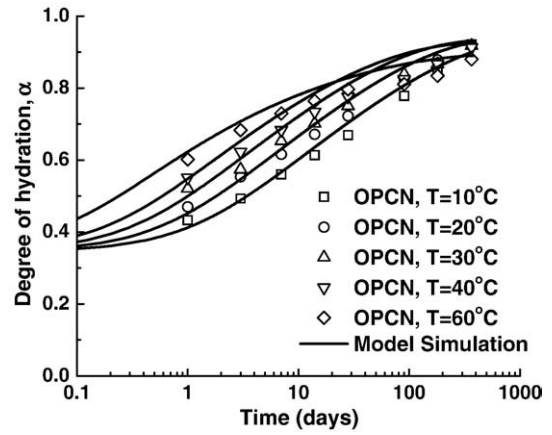


Fig. 9. Simulated and measured degree of hydration for cement #G (experimental data from [31]).

mentioned in Section 3.1, the function $s(\alpha, p)$ in Eq. (24) was calibrated using the experimental results for C_3S in [41]. The simulated and experimental results are compared in Fig. 12. In Fig. 13 the model reproductions of the degree of hydration for an ordinary Portland cement cured under pressure are compared with the experimental results of [42]. It can be seen that the model is capable of predicting the effect of applied hydrostatic pressure on cement hydration.

Hydration kinetics of three cements tested by Bentz et al. [46,14] and Hill et al. [35] are simulated using the proposed model. The experimental results of [46] exhibited the effect of curing conditions (saturated or sealed curing); those of [14] showed the effect of water-cement ratio; and those of [35] indicated the effect of curing temperature up to 90 °C (363 K), but the values of the degree of hydration were not provided. Such data are obtained by using the maximum heat output equation of Bogue [17], viz.

$$\alpha(t) \approx \frac{Q(t)}{Q_{\max}} \quad (33)$$

The material constants used in the simulation are obtained through Eqs. (29)–(32). Since the fineness of cement was not provided either, a value of 350 m²/kg is used by comparing the Blaine values of similar cements. The model reproductions are compared with the experimental results in Figs. 14–16, which show reasonably good agreement. Although the degree of hydration at the curing temperature of 90 °C [35] is over-estimated to a certain extent, the overall

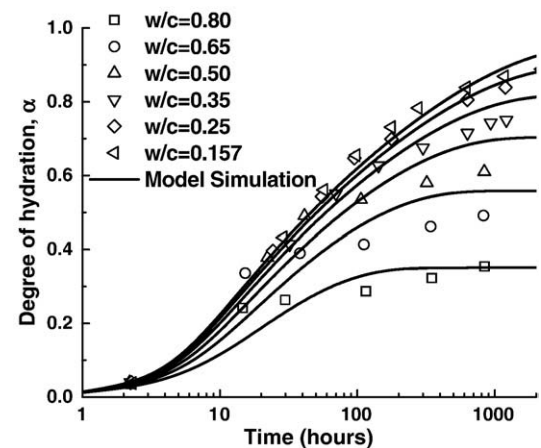


Fig. 10. Simulated and measured degree of hydration for cement #H (experimental data from [22]).

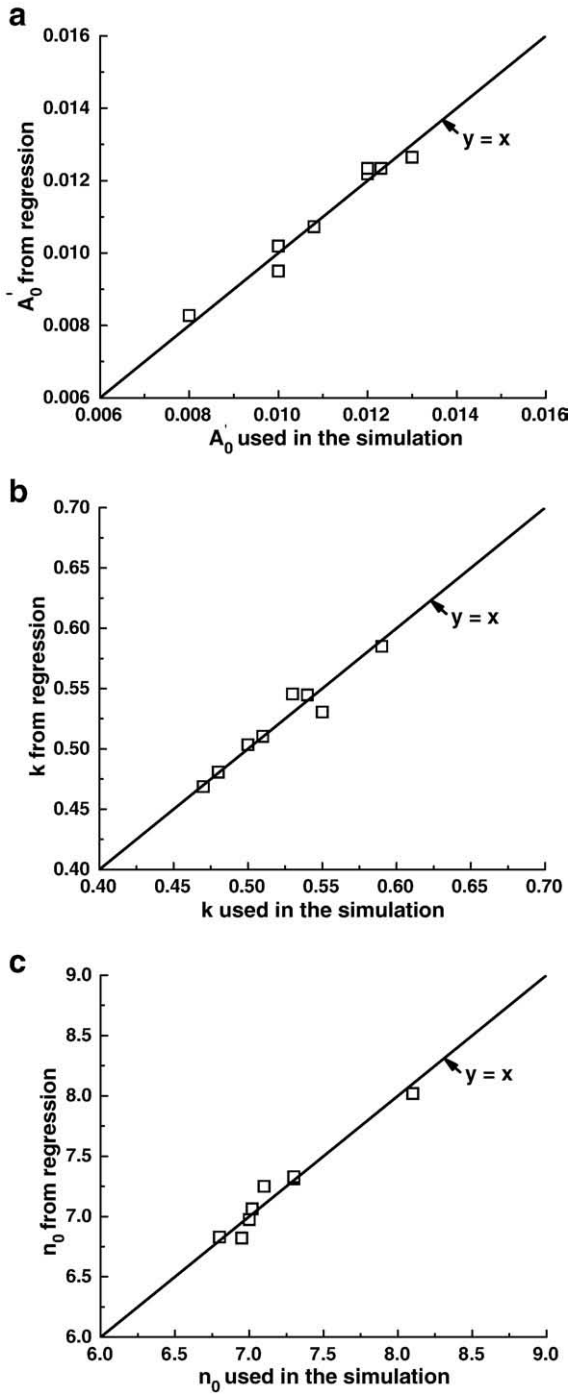


Fig. 11. Comparisons of the simulations with the regression values (a)—Eq. (30) for A_0 ; (b)—Eq. (31) for k ; (c)—Eq. (32) for n_0 .

prediction accuracy can be considered acceptable in view of the difficulties of conducting tests at elevated curing temperatures.

5.2. Model reproduction of adiabatic temperature rise

The exothermic behavior of cement hydration can be simulated by introducing the specific heat of cement paste, q_{paste} . van Breugel [3] proposed an equation for q_{paste} , which is a function of the degree of hydration α , curing temperature T , and water–cement ratio:

$$q_{paste} = \frac{M_{ce}}{\rho_{paste}} \cdot \left[\alpha \cdot q_{hce} + (1 - \alpha)q_{ace} + \frac{w}{c} \cdot q_w \right] \quad (34)$$

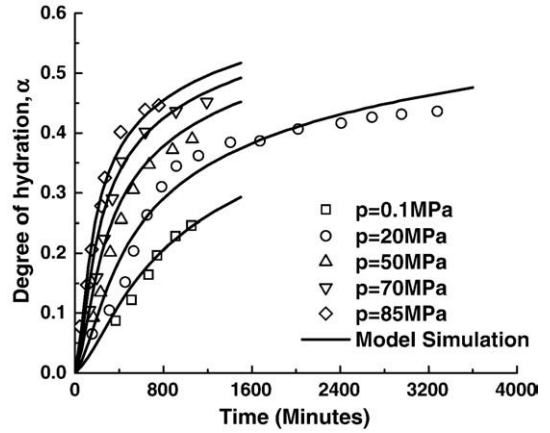


Fig. 12. Simulated and measured degree of hydration for C_3S under pressure (experimental data from [41]).

where M_{ce} [kg/m^3] is the cement content by mass in the paste; ρ_{paste} [kg/m^3] is the density of cement paste; q_{paste} , q_{ace} and q_w are the specific heats of cement paste, anhydrous cement, and water, respectively; q_{hce} [$kJ/(kg \cdot K)$] is the fictitious specific heat of the hydrated part of cement, which can be expressed as:

$$q_{hce} = 0.0084(T - 273) + 0.339 \quad (35)$$

The temperature rise, ΔT , can be written as:

$$\Delta T = \frac{\Delta\alpha \cdot Q_{max} \cdot M_{ce}}{\rho_{paste} \cdot q_{paste}} = \frac{\Delta\alpha \cdot Q_{max}}{\alpha \cdot q_{hce} + (1 - \alpha)q_{ace} + \frac{w}{c} \cdot q_w} \quad (36)$$

where $\Delta\alpha$ is the increase in the degree of hydration, and Q_{max} [kJ/kg] is the maximum heat of hydration. The values of the specific heat of cement and water are known to be $q_{ace} \approx 0.75$ $kJ/(kg \cdot K)$ and $q_w \approx 4.18$ $kJ/(kg \cdot K)$, respectively [3]. If concrete or mortar is concerned instead of cement paste, the specific heat and mass of aggregate should also be included in Eqs. (34) and (36).

The adiabatic tests for the CEM I 52.5 PM CP2 concrete by Bentz et al. [47] are reproduced using the proposed model to verify its capability to predict the adiabatic behavior of cementitious materials with different water–cement ratios. The material constants, except for the apparent activation energy E_α taken directly from [47], are obtained via Eqs. (30)–(32). The results are given in Fig. 17. It can be seen that the model predictions agree well with the experimental results.

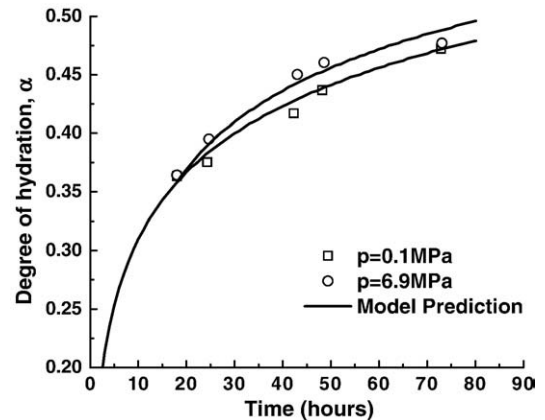


Fig. 13. Reproduced and measured degree of hydration for OPC under pressure (experimental data from [42]).

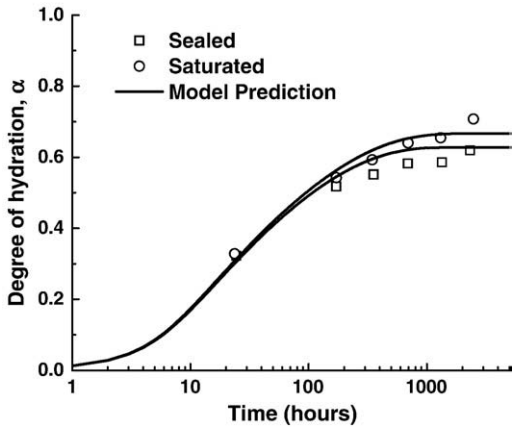


Fig. 14. Reproduced and measured degree of hydration for CCRL cement 115 under different curing conditions (experimental data from [46]).

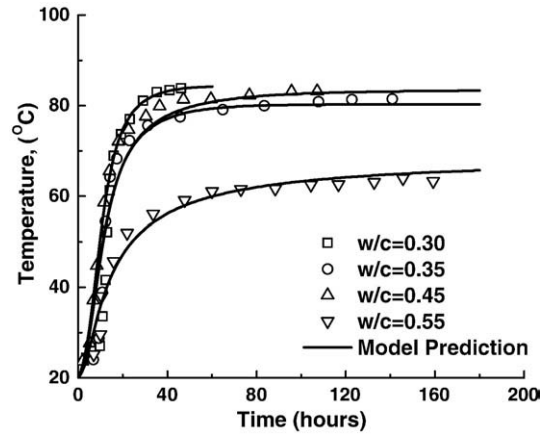


Fig. 17. Reproduced and measured adiabatic temperature changes for CEM I 52.5 PM CP2 cement with different water–cement ratios (experimental data from [47]).

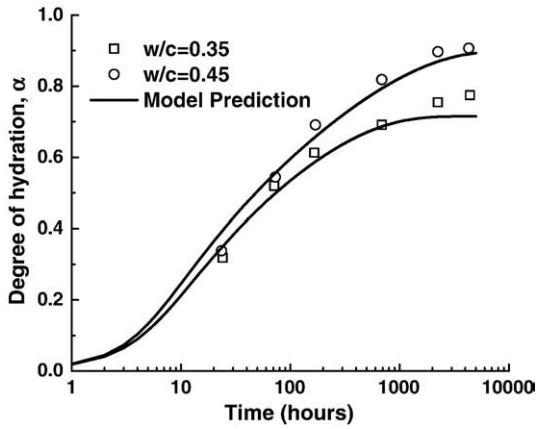


Fig. 15. Reproduced and measured degree of hydration for CCRL cement 152 with different water–cement ratios (experimental data from [14]).

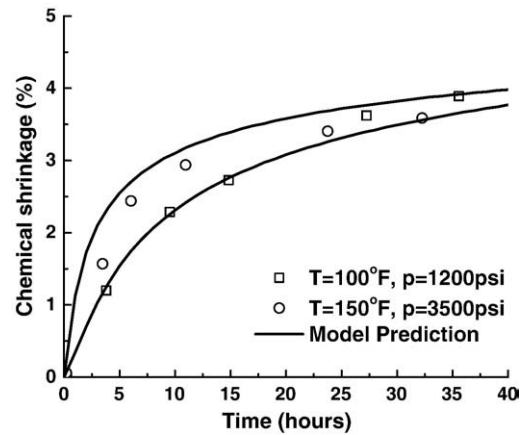


Fig. 18. Reproduced and measured chemical shrinkage for Class H cement at different temperatures and pressures (experimental data from [34]).

5.3. Model reproduction of chemical shrinkage

With the degree of hydration α , the chemical shrinkage of cement paste can be calculated, which according to [33], is approximated as:

$$v_{\text{chsh}}(\alpha) = \frac{(1 - v_n) \times \frac{w_n}{c} \times \alpha}{v_c + \frac{w}{c}} = \frac{0.25 \times 0.25 \times \alpha}{0.32 + \frac{w}{c}} \quad (37)$$

where $v_{\text{chsh}}(\alpha)$ is the chemical shrinkage; v_n ($\approx 0.75 \text{ cm}^3/\text{g}$) is the specific volume of the chemically bound water, which means that the

chemical shrinkage equals up to 25% of the volume of the chemically bound water; w_n is the mass of the chemically bound water; and v_c ($\approx 0.32 \text{ cm}^3/\text{g}$) is the specific volume of cement.

The chemical shrinkage tests by Chenevert and Shrestha [34], Justnes et al. [48,49] and Baroghel-Bouny et al. [45] are reproduced using the proposed model. It should be pointed out that the tests in [34] were conducted at high temperatures and high pressures. The material constants are again obtained via Eqs. (29)–(32). The

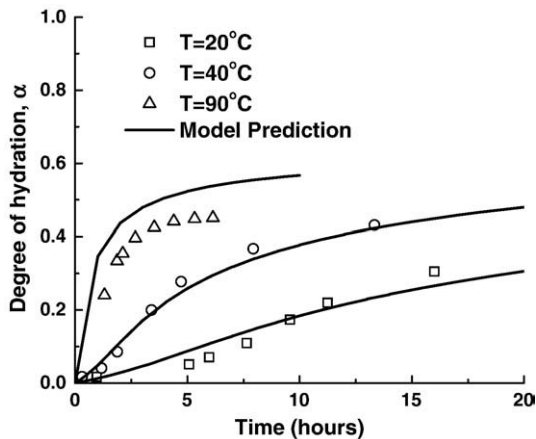


Fig. 16. Reproduced and measured degree of hydration for OPC at different temperatures (experimental data from [35]).

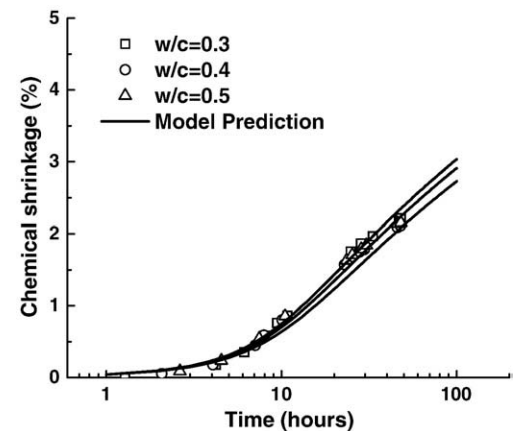


Fig. 19. Reproduced and measured chemical shrinkage for Class G cement with different water–cement ratios (experimental data from [48]).

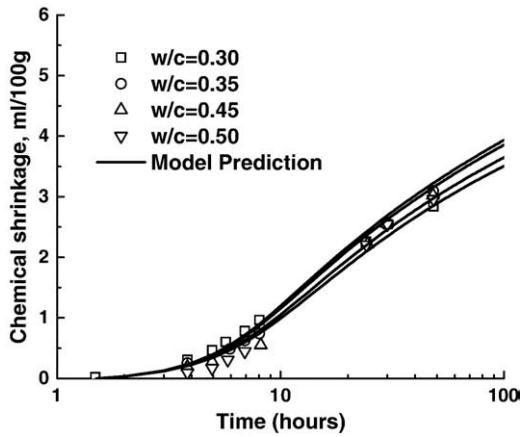


Fig. 20. Reproduced and measured chemical shrinkage for P30 k cement with different water–cement ratios (experimental data from [49]).

predicted and experimental results are compared in Figs. 18–22, which show acceptable agreement. The *Blaine* fineness was not provided in [34], hence a value of $300 \text{ m}^2/\text{kg}$ is adopted for the Class H oil well cement used in the tests by referring to the general fineness of this type of cement. Attention is directed to the model capacity of reproducing the behavior of oil well cements (Class G and Class H) under ambient conditions as well as downhole conditions of high temperature and high pressure. It should be noted that in the experiments the cement started to hydrate before the data were recorded. Therefore, values of the original degree of hydration in the model reproduction of the experimental results in [34] are not zero, but set as 0.04 at 38°C (100°F) and 0.12 at 66°C (150°F), respectively.

6. Summary and discussion

A hydration kinetics model for Portland cement has been proposed based on the thermo-chemical concepts of Ulm and Coussy [15]. The dominant mechanism of cement hydration is assumed to be the diffusion of free water through the layers of hydration products. The effects of chemical composition and fineness of cement, water–cement ratio, curing temperature and applied pressure are taken into account in this model. The influence of the chemical composition of cement is incorporated in the four material constants, k , A_0 , n_0 and E_{α} . The relationships between these material constants and the chemical composition of cement are calibrated.

The predictive capabilities of the model are demonstrated for various applications. The proposed hydration kinetics model is theoretically sound, easy to use and capable of predicting the hydration

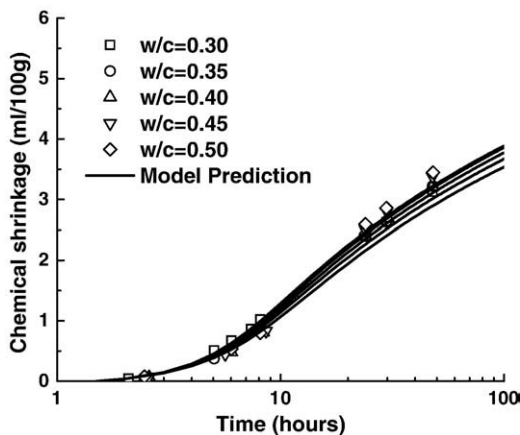


Fig. 21. Reproduced and measured chemical shrinkage for HS65 cement with different water–cement ratios (experimental data from [49]).

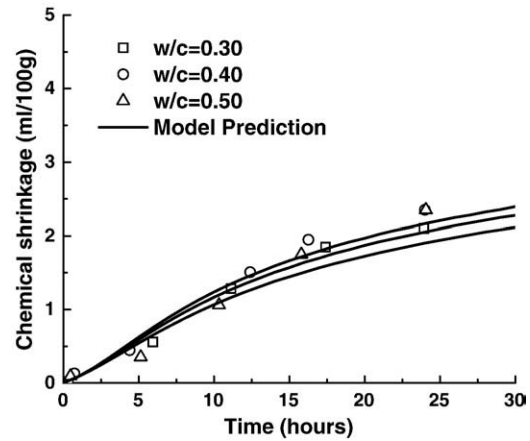


Fig. 22. Reproduced and measured chemical shrinkage for type I cement with different water–cement ratios (experimental data from [45]).

development of various cements under different curing conditions. In particular, the effects of elevated curing temperature and high applied pressure on hydration kinetics of cement can be reproduced. The proposed model can be used for different applications, such as the prediction of hydration kinetics, adiabatic temperature change and chemical shrinkage of cement paste.

Since only eight cements were used for the data regression analysis, the relationships between the three material constants (A_0 , k and n_0) and the chemical composition of cement may not be optimal. However, the trends of the relationships appear to have been captured. According to the available experimental observations, the initial reaction rate of C_4AF is the lowest, hence the material constant A_0 should be closely related to its content. The values of k and n_0 determine the overall reaction rate. The larger the value of k and the smaller the value of n_0 , the higher the reaction rate. It is well-known that C_3A and C_3S react faster, while C_2S reacts slower, hence the trends as given by Eqs. (31) and (32) are correct. The validity of using one single value of apparent activation energy E_{α} has been verified, but its dependence on the chemical composition and fineness of cement deserves further investigation.

The present study is focused on ordinary Portland cement without any mineral or chemical admixtures. However, it should be emphasized that this model is fundamentally capable of simulating the behavior of blended cements or cements with admixtures. Of course, in this case, the material constants would have to involve the effects of the replaced materials or the admixtures, but the model formulation would be similar.

The model's capacity of reproducing hydration kinetics of cement under curing conditions of high temperature and high pressure is demonstrated. However, the available experimental results under such conditions are very limited, therefore, the proposed formulas still need to be verified with more reliable experimental data.

Although it was reported in [3,8,27,28] that the particle size distribution of cement influences hydration kinetics to some extent, this influence is not considered in the proposed model. The assumption could lead to some discrepancy in the model simulation but since the trends of the particle size distribution curves of most generally used Portland cements are quite similar, it is considered to be acceptable. The predictive capacity of the model has demonstrated that this assumption does not introduce significant errors in this model for a wide variety of Portland cements.

It is also noteworthy that different methods to determine the degree of hydration can introduce considerable discrepancies among the obtained results. The methods commonly used to determine the degree of hydration vary from the uses of liberated heat of hydration, amount of chemically bound water, chemical shrinkage, amount of $\text{Ca}(\text{OH})_2$, to the approximations from the specific surface,

strength, or dielectric properties of cement. These differences between the methods to measure the degree of hydration should be borne in mind when modeling hydration kinetics for Portland cement.

Acknowledgements

The support of this study was provided by Halliburton Energy Services (HES), which is cordially appreciated. The enthusiastic help from Dr. Lewis Norman, Dr. Wolfgang Deeg, and many other personnel at Halliburton's Duncan Technology Center is gratefully acknowledged.

References

- [1] H.M. Jennings, S.K. Johnson, Simulation of microstructure development during the hydration of a cement compound, *Journal of the American Ceramic Society* 69 (11) (1986) 790–795.
- [2] D.P. Bentz, E.J. Garboczi, A digitized simulation model for microstructural development, in: S. Mindess (Ed.), *Advances in Cementitious Materials*, American Ceramic Society, Westville, Ohio, USA, 1989, pp. 211–226.
- [3] K. van Breugel, *Simulation of Hydration and Formation of Structure in Hardening Cement-Based Materials*, PhD Thesis, Delft University of Technology, The Netherlands (1991).
- [4] P. Navi, C. Pignat, Simulation of cement hydration and the connectivity of the capillary pore space, *Advanced Cement Based Material* 4 (2) (1996) 58–67.
- [5] K. Maekawa, R. Chaube, T. Kishi, *Modeling of Concrete Performance: Hydration, Microstructure Formation and Transport*, E&FN SPON, UK, London, 1999.
- [6] D.P. Bentz, Three-dimensional computer simulation of Portland cement hydration and microstructure development, *Journal of American Ceramic Society* 80 (1) (1997) 3–21.
- [7] J. Byfors, Plain concrete at early ages, Report FO 3:80, The Swedish Cement and Concrete Research Institute, CBI, Stockholm, Sweden, 1980, pp. 40–43.
- [8] T. Knudsen, Modeling hydration of Portland cement – the effect of particle size distribution, in: J.F. Young (Ed.), *Characterization and Performance Prediction of Cement and Concrete*, United Engineering Trustees, Inc., New Hampshire, USA, 1982, pp. 125–150.
- [9] P. Freiesleben Hansen, E.J. Pedersen, *Curing of Concrete Structures*, Draft DEB Guide to Durable Concrete Structures, Appendix 1, Comité Euro-International du Béton, Lausanne, Switzerland, 1985.
- [10] A.A. Basma, S.A. Barakat, S. Al-Oraimi, Prediction of cement degree of hydration using artificial neural networks, *ACI Materials Journal* 96 (2) (1999) 167–172.
- [11] H. Nakamura, S. Hamada, T. Tanimoto, A. Miyamoto, Estimation of thermal cracking resistance for mass concrete structures with uncertain material properties, *ACI Structural Journal* 96 (4) (1999) 509–518.
- [12] M. Cervera, R. Faria, J. Oliver, T. Prato, Numerical modeling of concrete curing, regarding hydration and temperature phenomena, *Computers and Structures* 80 (18–19) (2002) 1511–1521.
- [13] A.K. Schindler, K.J. Folliard, Heat of hydration models for cementitious materials, *ACI Materials Journal* 102 (1) (2005) 24–33.
- [14] D.P. Bentz, Influence of water-to-cement ratio on hydration kinetics: simple models based on spatial considerations, *Cement and Concrete Research* 36 (2) (2006) 238–244.
- [15] F.-J. Ulm, O. Coussy, Modeling of thermochemomechanical couplings of concrete at early ages, *Journal of Engineering Mechanics*, ASCE 121 (7) (1995) 785–794.
- [16] M. Cervera, J. Oliver, T. Prato, Thermo-chemo-mechanical model for concrete I: hydration and aging, *Journal of Engineering Mechanics*, ASCE 125 (9) (1998) 1018–1027.
- [17] R.H. Bogue, *The Chemistry of Portland Cement*, Reinhold Publishing Corp., New York, USA, 1947.
- [18] F.M. Lea, *The Chemistry of Cement and Concrete*, 3rd Ed. Chemical Publishing Company, Inc., USA, 1971.
- [19] R.L. Berger, A. Bentur, N.B. Milestone, J.H. Kung, Structural properties of calcium silicate pastes: I, effect of the hydrating compound, *Journal of the American Ceramic Society* 62 (7–8) (1979) 358–362.
- [20] J.I. Escalante-García, J.H. Sharp, Effect of temperature on the hydration of the main clinker phases in Portland cements: part I, neat cements, *Cement and Concrete Research* 28 (9) (1998) 1245–1257.
- [21] U. Danielson, Heat of hydration of cement as affected by water–cement ratio, Paper IV-S7, Proceedings of the 4th International Symposium on the Chemistry of Cement, Washington DC, USA, 1962, pp. 519–526.
- [22] J.H. Taplin, A method for following hydration reaction in Portland cement paste, *Australian Journal of Applied Sciences* 10 (1969) 329–345.
- [23] O.M. Jensen, Thermodynamic limitation of self-desiccation, *Cement and Concrete Research* 25 (1) (1995) 157–164.
- [24] R.H. Mills, Factors influencing cessation of hydration in water cured cement pastes, Special Report No. 90, Proceedings of the Symposium on the Structure of Portland Cement Paste and Concrete, Highway Research Board, Washington DC, USA, 1966, pp. 406–424.
- [25] R.R. Keienburg, Particle Size Distribution and Normal Strength of Portland Cement, PhD Thesis, Karlsruhe University, Germany (1976).
- [26] D.P. Bentz, C.J. Haecker, An argument for using coarse cements in high performance concretes, *Cement and Concrete Research* 29 (2) (1999) 615–618.
- [27] G. Frigione, S. Marra, Relationship between particle size distribution and compressive strength in Portland cement, *Cement and Concrete Research* 6 (1) (1976) 113–127.
- [28] A. Bezjak, An extension of the dispersion model for the hydration of Portland cement, *Cement and Concrete Research* 16 (2) (1986) 260–264.
- [29] W. Lerch, C.L. Ford, Long-term study of cement performance in concrete: chapter 3. Chemical and physical tests of the cements, *ACI Journal* 19 (8) (1948) 745–795.
- [30] K.O. Kjellsen, R.J. Detwiler, Reaction kinetics of Portland cement mortars hydrated at different temperatures, *Cement and Concrete Research* 22 (1) (1992) 112–120.
- [31] J.I. Escalante-García, Nonevaporable water from neat OPC and replacement materials in composite cements hydrated at different temperatures, *Cement and Concrete Research* 33 (11) (2003) 1883–1888.
- [32] A. Bentur, R.L. Berger, J.H. Kung, N.B. Milestone, J.F. Young, Structural properties of calcium silicate pastes: II, effect of the curing temperature, *Journal of the American Ceramic Society* 62 (7–8) (1979) 362–366.
- [33] T.C. Powers, T.L. Brownard, Studies of the physical properties of hardened Portland cement paste, *Bull. 22, Res. Lab. of Portland Cement Association*, Skokie, IL, USA, Reprinted from *J. Am. Concr. Inst. (Proc.)* vol. 43 (1947) 101–132, 249–336, 469–505, 549–602, 669–712, 845–880, 933–992.
- [34] M.E. Chenevert, B.K. Shrestha, Chemical shrinkage properties of oilfield cements, *SPE Drilling Engineering* 6 (1) (1991) 37–43.
- [35] J. Hill, B.R. Whittle, J.H. Sharp, M. Hayes, Effect of elevated curing temperature on early hydration and microstructure of composites, Proceedings of the Materials Research Society Symposium, vol. 757, 2003, pp. 699–703.
- [36] X. Xiong, K. van Breugel, Isothermal calorimetry study of blended cements and its application in numerical simulations, *HERON* 46 (3) (2001) 151–159.
- [37] P. Friessleben Hansen, E.J. Pedersen, Maturity computer for controlling curing and hardening of concrete, *Nordisk Betong* 1 (19) (1977) 21–25.
- [38] A.K. Schindler, Effect of temperature on hydration of cementitious materials, *ACI Materials Journal* 101 (1) (2004) 72–81.
- [39] D.M. Roy, G.R. Gouda, A. Bobrowsky, Very high strength cement pastes prepared by hot pressing and other high pressure techniques, *Cement and Concrete Research* 2 (3) (1972) 349–366.
- [40] D.M. Roy, G.R. Gouda, High strength generation in cement pastes, *Cement and Concrete Research* 3 (6) (1973) 807–820.
- [41] B. Bresson, F. Meducin, H. Zanni, Hydration of tricalcium silicates (C₃S) at high temperature and high pressure, *Journal of Materials Science* 37 (24) (2002) 5355–5365.
- [42] Q. Zhou, J.J. Beaudoin, Effect of applied hydrostatic stress on the hydration of Portland cement and C₃S, *Advances in Cement Research* 15 (1) (2003) 9–16.
- [43] D.P. Bentz, A three-dimensional cement hydration and microstructure program. I. Hydration rate, heat of hydration, and chemical shrinkage, NISTIR 5756, U.S. Department of Commerce, Washington DC, 1995.
- [44] G. Ye, Experimental Study and Numerical Simulation of the Development of the Microstructure and Permeability of Cementitious Materials, PhD Thesis, Delft University of Technology, The Netherlands (2001).
- [45] V. Baroghel-Bouny, P. Mounanga, A. Khelidj, A. Loukili, N. Rafai, Autogenous deformations of cement pastes Part II. W/c effects, micro–macro correlations, and threshold values, *Cement and Concrete Research* 36 (1) (2006) 123–136.
- [46] D.P. Bentz, K.A. Snyder, P.E. Stutzman, Hydration of Portland cement: the effects of curing conditions, Proceedings of the 10th International Congress on the Chemistry of Cement, vol. 2, 1997, Sweden.
- [47] D.P. Bentz, V. Waller, F. de Larrard, Prediction of adiabatic temperature rise in conventional and high-performance concretes using a 3-D microstructural model, *Cement and Concrete Research* 28 (2) (1998) 285–297.
- [48] H. Justnes, D. van Loo, B. Reyniers, P. Skalle, J. Sveen, E.J. Sellevold, Chemical shrinkage of oil well cement slurries, *Advances in Cement Research* 7 (26) (1995) 85–90.
- [49] H. Justnes, A. van Gemert, F. Verboven, E.J. Sellevold, Total and external chemical shrinkages of low w/c ratio cement pastes, *Advances in Cement Research* 8 (31) (1996) 121–126.